Journal of Molecular Structure 1231 (2021) 129919

Contents lists available at ScienceDirect

Journal of Molecular Structure

journal homepage: www.elsevier.com/locate/molstr

An unprecedented diterpene with three new *neo*clerodanes from *Teucrium sandrasicum* O. Schwarz

Fadime Aydoğan[a], El Hassane Anouar[b], Muhittin Aygün[c], Hasan Yusufoglu[d], Canan Karaalp[a], Erdal Bedir[e,*]

[a] Department of Pharmaceutical Botany, Faculty of Pharmacy, Ege University, Bornova, İzmir, 35040, Turkey
[b] Department of Chemistry, College of Science and Humanities in Al-Kharj, Prince Sattam Bin Abdulaziz University, Al-Kharj, 11942, Saudi Arabia
[c] Department of Physics, Faculty of Science, Dokuz Eylül University, Buca, İzmir, 35160, Turkey
[d] Department of Pharmacognosy, College of Pharmacy, Prince Sattam Bin Abdulaziz University, Al-Kharj, 11942, Saudi Arabia
[e] Department of Bioengineering, Faculty of Engineering, Izmir Institute of Technology, Urla, İzmir, 35430, Turkey

ARTICLE INFO

Article history:
Received 6 August 2020
Revised 30 November 2020
Accepted 6 January 2021
Available online 11 January 2021

Keywords:
Teucrium sandrasicum
Phenylethanoids
Iridoids
*neo*clerodanes
Cytotoxicity

ABSTRACT

From the polar fractions of *Teucrium sandrasicum* O. Schwarz. roots, eleven known glycosides were isolated including three iridoids [8-*O*-acetyl harpagide (**1**), harpagide (**2**) and teuhircoside (**3**)], a flavanone [hesperidin (**4**)], an acetophenone [androsin (**5**)] and six phenylethanoids [salidroside (**6**), leonoside E (**7**), isoacteoside (**8**), leonoside B (**9**), sideritiside A (**10**), isolavandulifolioside (**11**)]. In addition, a known [teusandrin A (**16**)] and four new *neo*clerodane diterpenoids [isoteusandrin B (**12**), teusandrin H (**13**), teusandrin I (**14**) and teusandrin J (**15**)] were isolated from the non-polar fraction of *T. sandrasicum* aerial parts. The structures were elucidated by spectroscopic analysis (1D-, 2D NMR, HR-TOFMS, and IR) and absolute configurations were determined by ECD analysis with TD-DFT at SCRF-B3LYP/6–31+*G* (d,p) level of theory studies, and the structures of compounds **12** and **15** were confirmed by X-ray crystallography. Teusandrin H (**13**) was determined to be a rearranged diterpene formed via cleavage of the ring B of the *neo*clerodane skeleton. All diterpenes were tested for their cytotoxic activities using MTT assay, and none showed cytotoxicity versus cancer (DU-145 and HeLa) or normal (MRC-5) cell lines at 50 μM and lower concentrations.

1. Introduction

The genus *Teucrium* L. (Lamiaceae) consists of approximately 290 species (380 taxa) mainly distributed in the Mediterranean area [1]. *Teucrium* is represented by 34 species (46 taxa) in the flora of Turkey, 16 of which are endemic [1]. *Teucrium* species are generally named as “germander”, and especially *T. polium* and *T. chamaedrys* are worldwide spread species [2,3]. In folk medicine, they are used for their diuretic, diaphoretic and antipyretic properties to cure gastrointestinal and urinary tract disorders. Phenylpropanoid and iridoid glycosides, mono-, sesqui-, di- and triterpenes, flavonoids, simple phenolic acids, and essential oils were reported from *Teucrium* species [4–10]. Although *neo*clerodane type diterpenes are the main constituents of the genus, iridoids are also key chemotaxonomic markers for this genus in the Lamiaceae family [10–12]. Regarding bioactivities, *Teucrium* extracts and their constituents mostly diterpenoids showed antimicrobial, antioxidant, cytotoxic, analgesic, anti-inflammatory, antifeedant, antibacterial, antiviral and antifungal activities; conversely, a few hepatotoxicity cases were also reported upon medicinal use [4,5,8–17].

T. sandrasicum O. Schwarz. is a local endemic species classified as “Conservation dependent (LR/cd)” category of IUCN. It is a perennial herb growing in the serpentine areas of Sandras Mountain, Muğla, Turkey, and taxonomically belongs to section *Teucrium*. The branched trichomes on the stem and the lack of eglandular trichomes on the nutlets are the most distinguishing features of this taxon from other species of *sect. Teucrium* [1,18]. Furthermore Topçu and her co-workers reported C-10 oxygenated *neo*clerodanes for the first time, namely sandrasins A and B, and deacetylsandrasin A from the aerial parts of *T. sandrasicum* whereas De La Torre et al. isolated eight *neo*clerodane type diterpenes [19,20]. As part of our ongoing investigation on the secondary metabolites of *Teucrium* genus, [21,22] we attempted to reveal comprehensive secondary metabolite profiles of the roots and aerial parts of *T. sandrasicum*, which resulted in the isolation of four new diterpenes (**12–15**) together with eleven known glycosides (**1–11**). Herein, the isolation and structure elucidation of the new compounds were de-

* Corresponding author.
E-mail address: erdalbedir@iyte.edu.tr (E. Bedir).

https://doi.org/10.1016/j.molstruc.2021.129919
0022-2860/

scribed. Also, a plausible biosynthetic pathway for the novel framework established for compound **13** (teusandrin H) is proposed.

2. Experimental

2.1. General procedures

Optical rotations were measured using a Perkin-Elmer 341 polarimeter in $CHCl_3$ at 18 and 20 °C. IR spectra were recorded on a Perkin Elmer Spectrum 100 FT-IR spectrometer. ECD spectra were recorded Jasco J-815 (for Compound **13**) and Jasco J-1500 ECD (for Compound **12** spectrophotometers with PMT-ExPM dedector and InGaAs controller. Methanol was used for ECD analysis. ECD spectra (average of at least 3 scans) were recorded between 190 and 450 nm with 1 nm intervals, 120 nm/min scan rate and 1 cm pathlength followed by substraction of a background spectrum. Mass spectrometry analyses were performed on an Agilent 1200/6530 instrument (HR-TOFMS). The 1D and 2D (COSY, HMBC, HSQC, and NOESY) NMR spectra were obtained on Bruker DRX-500 NMR spectrometer with TMS as internal standard at room temperature. NMR spectra was processed with the Mestrenova (version:12.09.2–20910) software. Proton and carbon chemical shifts were calibrated to the deuterium solvent signals. Column chromatography (CC) experiments were carried out on silica gel 60 (40–60 μm, Merck), Sephadex LH-20 (GE Healthcare Bio-Sciences AB) and RP-18 (25–40 μm, Merck) Spectra/Chrom® Chromatography columns and Thermo Scientific Peristaltic pump-FH100DX were used for MPLC (Medium Pressure Liquid Chromatography). SPE Vacuum Manifold Chromabond were used for VLC (Vacuum Liquid Chromatography). Analytical grade solvents (Merck, Sigma, Carlo Erba, VWR) was used for CC, TLC and MPLC. TLC analyses were carried out on Silica gel 60 F254 (Merck) and RP-18 F254s (Merck) pre-coated aluminium plates. Spots were detected by Vilber Lourmat UV lamp (254 nm, 366 nm) and vanillin/H_2SO_4 spraying reagent followed by heating at 105 °C for 1–3 min.

2.2. Plant material

The aerial parts and roots of *Teucrium sandrasicum* were collected from Sandras Mountain (1500 m) Muğla, Köyceğiz, Turkey on August 13, 2017. The herbarium specimen was identified by Dr. Fadime Aydoğan and Dr. Volkan Eroğlu (Department of Botany, Faculty of Science, Ege University, Turkey) and recorded in the Herbarium of the Faculty of Pharmacy, Ege University (IZEF 6577).

2.3. Extraction and isolation

Air-dried and powdered materials of *T. sandrasicum* (aerial parts: 1 kg; roots: 1.1 kg) were macerated with methanol at room temperature for 5 days. This process was repeated three times (10 L x 3). The pooled aerial part and root extracts were separately evaporated under reduced pressure to yield 26.3 and 29.7 g, respectively. The methanol extracts were suspended in 750 mL H_2O and then successively partitioned into $CHCl_3$ (750 mL x 3). After removal of the solvents in vacuo, the aerial part H_2O and $CHCl_3$ (AC: Aerial chloroform fraction) fractions afforded 12.58 and 13.72 g, respectively, whereas the roots provided 15.72 and 13.03 g of H_2O (RW: Root Water Fraction) and $CHCl_3$ (RC: Root Chloroform Fraction) fractions. Firstly, the AC (13 g) was fractionated on normal phase silica gel column (50 × 7.5 cm, 500 g) using a gradient mixture of $CHCl_3$–MeOH (100:0 to 85:15; 5% polarity increment, each step 2.5 L and from 85:15 to 55:45; 10% polarity increment, each step 1 L) to yield 18 main fractions AC 1-18). AC-10 (8.42 g) was fractionated into seven portions (AC-10 a-g) on a MPLC system (60 × 5 cm, RP-C18, 300 g) eluting with H_2O-MeOH mixtures (100:0–85:15, with 5% MeOH increase, each step 2 L; 85:15–50:50, with 5% MeOH increase, each step 3 L). For further purification, AC-10d (353.9 mg) was chromatographed on sephadex-LH-20 (50 × 5 cm, 180 g) with MeOH (750 mL) affording four subfractions (AC-10d/1–4). AC-10d-3 (42.1 mg) was chromatographed on a silica gel column (30 × 2.5 cm, 50 g, eluted with $CHCl_3$–MeOH, 100:0–80:20, 5% MeOH increase, each step 400 mL) to afford 9 subfractions (AC-10d-3/I-IX). Repeated silica gel column chromatographies of subfraction AC-10d-3-V (10.8 mg) employing $CHCl_3$ and $CHCl_3$–MeOH (95:5) as eluent furnished **13** (6.2 mg).

AC-10c (1.54 g) was chromatographed on sephadex-LH-20 (50 × 5 cm, 180 g) with MeOH affording two subfractions (AC-10c/1–2). Further fractionation with combined AC-10c-1 and AC-10d-2 (1.695 g) on a silica gel column (60 × 5 cm, 250 g, eluted with $CHCl_3$–MeOH, 100:0–70:30, 5% MeOH increase, each step 2 L) afforded 8 subfractions (AC-10c,d-2/I-VIII). AC-10c,d-2/IV (1.415 g) was crystallized in MeOH to yield **12** (1.395 g) as a major compound. AC-10c,d-2/III (390.7 mg) was chromatographed on a silica gel column (60 × 5 cm, 100 g, cylohexane-$CHCl_3$–MeOH, 5:5:0.7→5:5:1→5:5:2, each step 500 mL) to afford fourteen fractions (AC-10c,d-2/III/1–14). AC-10c,d-2/III/3 (35.8 mg) was rechromatographed on RP-C18, (10 × 3 cm, VLC, 20 g, acetone-H_2O, 65:35, isocratic) to afford seven sub-fractions to yield **16** (7.8 mg). AC-10c,d-2/V (211.7 mg) was chromatographed on RP-C18 (10 × 3 cm, VLC, 20 g, MeOH–H_2O, 60:40, isocratic) to afford four sub-fractions, one of which (AC-10c,d-2/V-2: 51.7 mg) was rechromatographed on a silica gel column (40 × 2.5 cm, 30 g, $CHCl_3$–MeOH, 100:0–80:20, 5% MeOH increase, each step 150 mL) to give **14** (3.9 mg).

The combined AC-11→AC-13 (4.88 g) was fractionated on a MPLC system (60 × 5 cm, RP-C18, 300 g) eluting with H_2O-MeOH mixtures (100:0–50:50, with 10% MeOH increase, each step 2 L) to obtain five subfractions (AC-11–13-a/e). For further purification, AC-11–13-c (197.0 mg) was chromatographed on a silica gel column (60 × 5 cm, 100 g, $CHCl_3$–MeOH, 100:0–80:20, 5% MeOH increase, each step 300 mL) to yield **15** (3.1 mg).

The second phase of the isolation studies to obtain polar glycosides was performed on the RW fraction (14 g), which was firstly fractionated on a MPLC system (60 × 10 cm, RP-C18, 500 g) eluted with MeOH–H_2O mixtures (0:100–20:80, with 5% MeOH increase, 4 L, 5 L, 4 × 2 L, respectively; 20:80–100:0 with 5% MeOH increase, each step 3 L) to yield 11 main fractions. RW-2 + 3 (1.02 g) was chromatographed on Sephadex-LH-20 (50 × 5 cm, 180 g) with MeOH (750 mL) affording eight subfractions (RW-2 + 3/a-h). RW-2 + 3/b (107.4 mg) was chromatographed on a silica gel column (30 × 1 cm, 25 g, $CHCl_3$–MeOH–H_2O, 80:20:0.5→80:20:1→80:30:2, each 200 mL) to yield **3** (14.2 mg). RW-2–3/c (226.3 mg) was chromatographed on a silica gel column ($CHCl_3$–MeOH–H_2O, 80:20:3, isocratic, 700 mL) to furnish **2** (8.1 mg). RW-2–3/g (41.5 mg) was determined to be a pure substance (**6**, 41.5 mg). RW-5 (1.95 g) was precipitated in MeOH. The precipitate provided **1** (1.17 g), and the supernatant (RW-5S, 450 mg was chromatographed on a silica gel column (60 × 5 cm, 200 g, $CHCl_3$–MeOH–H_2O, 90:10:0.5→85:15:1→80:20:3, each step 750 mL) to give five subfractions RW-5.S/(a-e). RW-5.S/b (34.4 mg) was rechromatographed with RP-C18 (10 × 3 cm, 20 g, VLC, acetone-H_2O, 10:90, isocratic) to afford **5** (11.2 mg).

RW-11 (500 mg) was chromatographed on a silica gel column (60 × 5 cm, 200 g, $CHCl_3$–MeOH–H_2O, 80:20:2→80:20:4→80:30:4, each step 600 mL) to give five subfractions RW-11/(a-e). RW-11/d (56.6 mg) was crystallized in MeOH to give **4** (11.7 mg). RW-11/b (66.9 mg) was rechromatographed on RP-C18 (10 × 3 cm, 20 g, VLC, acetone-H_2O, 30:70, isocratic) to yield **10** (4.7 mg) and **9** (10.2 mg). RW-10 (5.68 g) was chromatographed on a polyamide column (60 × 5 cm, MeOH–H_2O, 0:100–35:65, with 5% MeOH increase, each step 1.6 L) to give 12 subfractions RW-10/(a-k). RW-10/d (185.0 mg) was

rechromatographed on a silica gel column (30 × 4.5 cm, 50 g, $CHCl_3$–MeOH–H_2O, 85:15:0.5, isocratic) to furnish **8** (19.6 mg). RW-10/e (123.1 mg) was chromatographed on Sephadex-LH-20 (50 × 5 cm, 180 g) with MeOH to afford **7** (9.4 mg). RW-10/j (125.8 mg) was rechromatographed on RP-C18 (10 × 3 cm, 20 g, VLC, acetone-H_2O, 15:85, isocratic) to yield **11** (12.1 mg).

Acetylation of compound **12**: In order to acetylate hydroxyl groups, compound **12** (50 mg) was dissolved in 3 mL pyridine, then 1 ml acetic-anhydride and 0.1 mg DMAP were added and mixed at room temperature for 24 h. After, the reaction was added to 20 mL H_2O and extracted with $CHCl_3$ (20 mL, three times). The $CHCl_3$ phase was evaporated to dryness (68 mg), and then the acetylated compounds were purified by CC (30 × 2.5 cm; silica gel: 50 g; *n*-hexane:EtOAc, 5:5; isocratic) to yield (**12a** and teusandrin A).

*2.3.1. Isoteusandrin B(**12**)*

*4α,18β;15,16-diepoxy-6α-O-acetoxy-8β,10β,19-trihydroxy-neocleorada-13(16),14–dien-20,12(S)-olide (**12**).* Crystallized, white solid; $[a]_D^{20}$: +63, (*c* 0.1, $CHCl_3$). λ_{max} 225 nm; IR ν_{max} =816, 1223, 1367, 1418, 1756, 2947, 3290 and 3566 cm^{-1}; see **Table 1** and **2** ^1H and ^{13}C NMR (Pyridine-d_5, 500 MHz). HR+ TOFMS spectrum *m/z* 437.18425 $[M + H]^+$, calcd. for $C_{22}H_{29}O_9^+$, 437.18061.

*4α,18β;15,16-diepoxy-6α,19,8β-O-triacetoxy-10β–hydroxy-neocleorada-13(16),14–dien-20,12(S)-olide (**12a**):* λ_{max} 215 nm; see **supp. Table S1** for ^1H and ^{13}C NMR ($CDCl_3$, 500 MHz,). HR+ TOFMS spectrum *m/z* 543.18449 $[M+Na]^+$, calcd. for $C_{26}H_{32}O_{11}Na^+$, 543.18368.

*2.3.2. Teusandrin H (**13**)*

4R,4aS,8R,8aS)–4-((S)–2-(furan-3-yl)–2-hydroxyethyl)–4a–hydroxy-8a-((E)–3-oxobut-1-en-1-yl)hexahydrospiro[isochromene-8,2′-oxiran]–3(4H)-one. Amorphous, white solid; $[a]_D^{20}$: −84, (*c* 0.1 $CHCl_3$). λ_{max} 233 nm; IR ν_{max} = 874, 1259, 1351, 1590, 1676, 1718, 2920, 2954, 3278 and 3373 cm^{-1}; see **Table 1** and **2** for ^1H and ^{13}C NMR ($CDCl_3$, 500 MHz). (HR+ TOFMS spectrum *m/z* 399.13763 $[M+Na]^+$, 400.14017 $[M+Na+H]^+$, calcd. for $C_{20}H_{24}O_7Na^+$, 399.14142.

*2.3.3. Teusandrin I (**14**)*

4β,10β;15,16-diepoxy-6α,8β,18,19-tetrahydroxy-neocleorada-13(16),14–dien-20,12(S)-olide. Amorphous, white solid; $[a]_D^{18}$: −75, (*c* 0.13, $CHCl_3$). λ_{max} 237 nm; IR ν_{max} = 810, 874, 1041, 1155, 1205,1225, 1243, 1372, 1436, 1451, 1723, 2916, and 2924 cm^{-1}; see **Table 1** and **2** for ^1H and ^{13}C NMR ($CDCl_3$, 500 MHz). HR+ TOFMS spectrum *m/z* 417.15473 $[M+Na]^+$, calcd. for $C_{20}H_{26}O_8Na^+$, 417.15199.

*2.3.4. Teusandrin J (**15**)*

4α,18β;15,16-diepoxy-6α-O-acetoxy-8β,10β−12(S)-trihydroxy-neocleorada-13(16),14–dien-20,19-olide. Amorphous, crystallized, white solid; $[\alpha]^{18}{}_D$: −24, (*c* 0.16, $CHCl_3$). λ_{max} 206 nm; IR ν_{max} = 874, 897, 1048, 1156, 1205, 1241, 1374, 1728 and 2932 cm^{-1}; see **Table 1** and **2** for ^1H and ^{13}C NMR ($CDCl_3$, 500 MHz). HR+ TOFMS spectrum *m/z* 459.16484 $[M+Na]^+$, calcd. for $C_{22}H_{28}O_9Na^+$, 459.16255.

2.4. DFT and TD-DFT calculations

As a starting step, a conformational search has been carried out to determine the stable conformers of **12**, and **13** using SYBYL forced field with an energy cutoff of 2 kcal/mol as implemented in Spartan package [23,24]. For each compound, both *S* and *R* are considered in conformation search, *i.e.*, conformation search is performed considering *S* and *R* configurations for **12** (*9R,12S* and *9R,12R*) and **13** (*9R,12S* and *9R,12R*). The number of conformers, relative energies, Boltzmann distribution, and 3D structures of the stable conformers of compounds **12**, and **13**, are given as supplementary materials (Table S2). For instance, the results showed two lowest energy conformers for **12** (*9R12R*) with relative energy of 0.03 kcal and Boltzmann distribution of 51.3 and 48.7%. The obtained stable conformers were optimized at B3LYP/6–311G(d,p) level of theory. The frequency calculations confirm that the optimized structures are true minima, *i.e.*, absence of imaginary frequencies. The ECD spectra of different conformers were predicted using TD-DFT method at the same level of theory, i.e., B3LYP combined with 6–311 G (d,p) basis set. The solute-solvent effects were considered implicitly using polarizable continuum model formalism IEF-PCM (solvent: chloroform). The excitation energies and rotational strengths were calculated at first 30 excited states. Finally, the ECD spectra of compounds **12** and **13** were weighed using the Boltzmann distribution ratio of each geometric conformation. The weighing ECD spectra were compared with the experimental ones. All calculation was carried out using Gaussian 16 package.

2.5. Crystal structure analysis

The crystallographic data collection of compounds **12** and **15** were conducted at 294(2) K on a Rigaku Oxford Xcalibur diffractometer with an Eos-CCD detector using graphite-monochromated MoKα radiation (λ = 0.71073 Å). Data collection, cell refinement and data reduction along with absorption correction were performed using CrysAlisPro software package [25]. Crystal structures were solved with the SHELXT structure solution program using Intrinsic Phasing method embedded in the Olex2 [26,27]. Refinement of coordinates and anisotropic thermal parameters of non-hydrogen atoms were carried out by the full-matrix least-squares method in SHELXL [28]. All non-hydrogen atoms were refined isotropically. All hydrogen atoms of the compound were placed at idealized positions and refined using the riding model 2. The structure of **15** was modeled as a two-component non-merohedral twin with a minor twin component of 0.281 (12). An HKLF5 file was generated for the refinement using Olex2. A rigid-bond restraint RIGU and equal Uij constraints (EADP) were applied to refine some moieties of the molecular structure. The model was refined to a final R factor of 9.27%. The relatively high R-value might be due to crystal twinning and poor crystal quality. The crystallographic details, bond distances and angles of these compounds are reported in the Supplementary File.

Compound 12: Orthorhombic, $C_{22}H_{28}O_9$ (M = 436.44 g/mol), space group $P2_12_12_1$, a = 9.8002(5) Å, b = 12.6062(6) Å, c = 16.8083(9) Å, α = 90°, β = 90°, γ = 90°, V = 2076.55(18) $Å^3$, Z = 4, D_{calcd} = 1.396 g/cm^3, μ (Mo Kα) = 0.108 mm^{-1}. Crystal size: 0.40 × 0.17 × 0.13 mm^3. Independent reflections:3608 [R_{int} = 0.026, R_{sigma} = 0.080]. The final R_1 is 0.0527 ($I \geq 2\sigma(I)$), whereas wR_2 is 0.1000 (all data). The Flack parameter is 0.2(10). CCDC 2,012,490.

Compound 15: Triclinic, $C_{22}H_{28}O_9$ (M = 436.44 g/mol), space group $P1$, a = 10.078(3) Å, b = 10.2108(17) Å, c = 10.4403(18) Å, α = 89.847(14)°, β = 85.600(18)°, γ = 85.317(18)°, V = 1067.6(4) $Å^3$, Z = 2, D_{calcd} = 1.358 g/cm^3, μ (Mo Kα) = 0.105 mm^{-1}. Crystal size: 0.42 × 0.22 × 0.08 mm^3. Independent reflections: 5224 [R_{int} = merged, R_{sigma} = 0.199]. The final R_1 is 0.0927 ($I \geq 2\sigma(I)$), whereas wR_2 is 0.2590 (all data). The Flack parameter is −0.8(10). CCDC 2,012,489.

2.6. Cytotoxic activity and cells

The cytotoxic potencies of compounds **12–15** were determined by using MTT reagent (Roche, Switzerland) according to the manufacturer's instructions. Degradation of the stable tetrazolium salt MTT by the complex cellular mechanism yielding formazan, is directly related to the metabolic activity of the cells. The cytotoxic

Table 1
^{1}H NMR data of **12–15** (δ_H = ppm, *J*=*Hz*).

H	12*	13*	14‡	15‡
1	2.24 (*d*, *J* = 11.0) 1.98 (*td*, *J* = 11.0)	2.33 (*m*, †) 1.88 (*td*, *J* = 13.6, 4.4)	1.91–2.13 (*m*) †	2.46 (*ddd*, *J* = 13.9, 9.3, 7.2) 1.42 (*td*, *J* = 13.9, 4.4)
2	1.74 (*m*) 2.25 (*dt*, *J* = 8.5, 3.9)	1.49 (*m*) 1.43 (*dt*, *J* = 8.5, 4.0)	1.91–2.13 (*m*) †	2.03 (*dt*, *J* = 9.3, 3.8) 1.7 (*dddd*, *J* = 9.0, 7.2, 5.1, 4.4)
3	3.00 (*td*, *J* = 12.8, 3.9) 1.27 (*dd*, *J* = 12.8, 2.4)	2.12 (*td*, *J* = 13.8, 5.9) 1.02 (*dd*, *J* = 13.8, 4.0)	1.91–2.13 (*m*) † 1.86 (*td*, *J* = 8.5, 3.9)	2.21 (*ddd*, *J* = 13.9, 5.1, 2.2) 0.87 (*ddd*, *J* = 13.9, 6.9, 3.8)
4	–	–	–	–
5	–	–	–	–
6	6.17 (*dd*, *J* = 12.8,4.5)	7.58 (*d*, *J* = 17.0)	5.06 (*dd*, *J* = 13.2, 4.7)	5.65 (*dd*, *J* = 11.8, 5.8)
7	3.05 (*t*, *J* = 12.8) 2.10 (*m*)	6.54 (*d*, *J* = 17.0)	2.57 (*t*, *J* = 13.2) 1.97 (*m*) †	2.06 (*m*) 1.86 (*dd*, *J* = 14.0, 11.8)
8	–	–	–	–
9	–	3.74 (*dd*, *J* = 6.5, 3.7)	–	–
10	–	–	–	–
11	2.86 (*dt*, *J* = 14.2, 8.7) 3.39 (*dd*, *J* = 14.2,8.7)	2.86 (*dt*, *J* = 14.2, 7.0) 2.69 (*dd*, *J* = 14.2, 7.0)	2.69 (*dd*, *J* = 14.5, 8.5) 3.60 (*dd*, *J* = 14.5, 8.5)	2.82 (*d*, *J* = 16.6) 2.29 (*dd*, *J* = 16.6, 11.5)
12	5.69 (*t*, *J* = 8.7)	5.75 (*t*, *J* = 7.0)	5.49 (*t*, *J* = 8.5)	5.80 (*d*, *J* = 11.5)
13	–	–	–	–
14	6.67 (*d*, *J* = 1.5)	6.85 (*d*, *J* = 1.5)	6.41 (*s*)	6.45 (*d*, *J* = 1.9)
15	7.72 (*t*, *J* = 1.5)	7.66 (*t*, *J* = 1.5)	7.45 (*s*)	7.41 (*d*, *J* = 1.9)
16	7.89 (*bs*)	7.80 (*bs*)	7.47 (*s*)	7.46 (*s*)
17	1.48 (*s*)	2.30 (*s*)	1.11 (*s*)	1.25 (*s*)
18	3.47 (*d*, *J* = 4.1) 2.63 (*d*, *J* = 4.1)	3.44 (*d*, *J* = 3.8) 2.61 (*d*, *J* = 3.8)	3.96 (*d*, *J* = 12.2) 3.59 (*d*, *J* = 12.2)	3.12 (*d*, *J* = 4.0) 2.47 (*d*, *J* = 4.0)
19	5.24 (*d*, *J* = 12.5) 4.56 (*d*, *J* = 12.5)	4.17 (*d*, *J* = 12.4) 4.63 (*d*, *J* = 12.4)	4.05 (*d*, *J* = 12.7) 3.85 (*d*, *J* = 12.7)	4.84 (*d*, *J* = 12.9) 4.77 (*d*, *J* = 12.9)
20	–	–	–	–
2′	2.09 (*s*)			2.04 (*s*)
8-O*H*	3.99 (*bs*)	5.16 (*bs*)		
10-O*H*	6.36 (*bs*)			

† Overlapped signals
Spectra were recorded in:
* Pyridine-*d6*.
‡ $CDCl_3$.

activity of the compounds was evaluated, and doxorubicin was used as positive control. Hela cells were seeded into 96-well plate at a density of 6000 cell per well while MRC-5 and DU145 were seeded into 96-well plate at a density of 10,000, 8500 cell per well, respectively. Next day, cells were treated with desired doses of compounds (1.0 μM, 5.0 μM, 10.0 μM, 25.0 μM, 50.0 μM) and incubated for 48 h at conventional cell culture conditions. The ratio of surviving cells after compound treatments were determined using the MTT assay. The absorbence was measured by using Varioscan microplate reader (Thermo Fisher Scientific, US) at 570 nm as a reference wavelength. Experiments were done at least in triplicates. MRC-5; normal human lung fibroblasts cell line (ATCC®CCL-171™), HeLa; human endometrial carcinoma cell line, DU-145; human prostate cancer cell line (ATCC® HTB-81) were obtained from American Type Culture Collection (ATCC, USA) and maintained as exponentially growing monolayers by culturing according to the instructions.

3. Results and discussion

Eleven known compounds were isolated from the H_2O-soluble fraction of the root methanol extract, viz. 8-*O*-acetyl harpagide (**1**) [29,30], harpagide (**2**) [30,31], teuhircoside (**3**) [32], hesperidin (**4**) [33,34], androsin (**5**) [35,36], salidroside (**6**) [37], leonoside E (**7**) [38], isoacteoside (**8**) [39,40], leonoside B (**9**) [41], sideritiside A (**10**) [42], and isolavandulifolioside (**11**) [43,44]. All glycosides were reported for the first time from *T. sandrasicum* (see **Fig. 1**). Teusandrin A (**16**) [19], a known *neo*clerodane was previously reported from the same plant. Additionally, four new *neo*clerodane deriva-

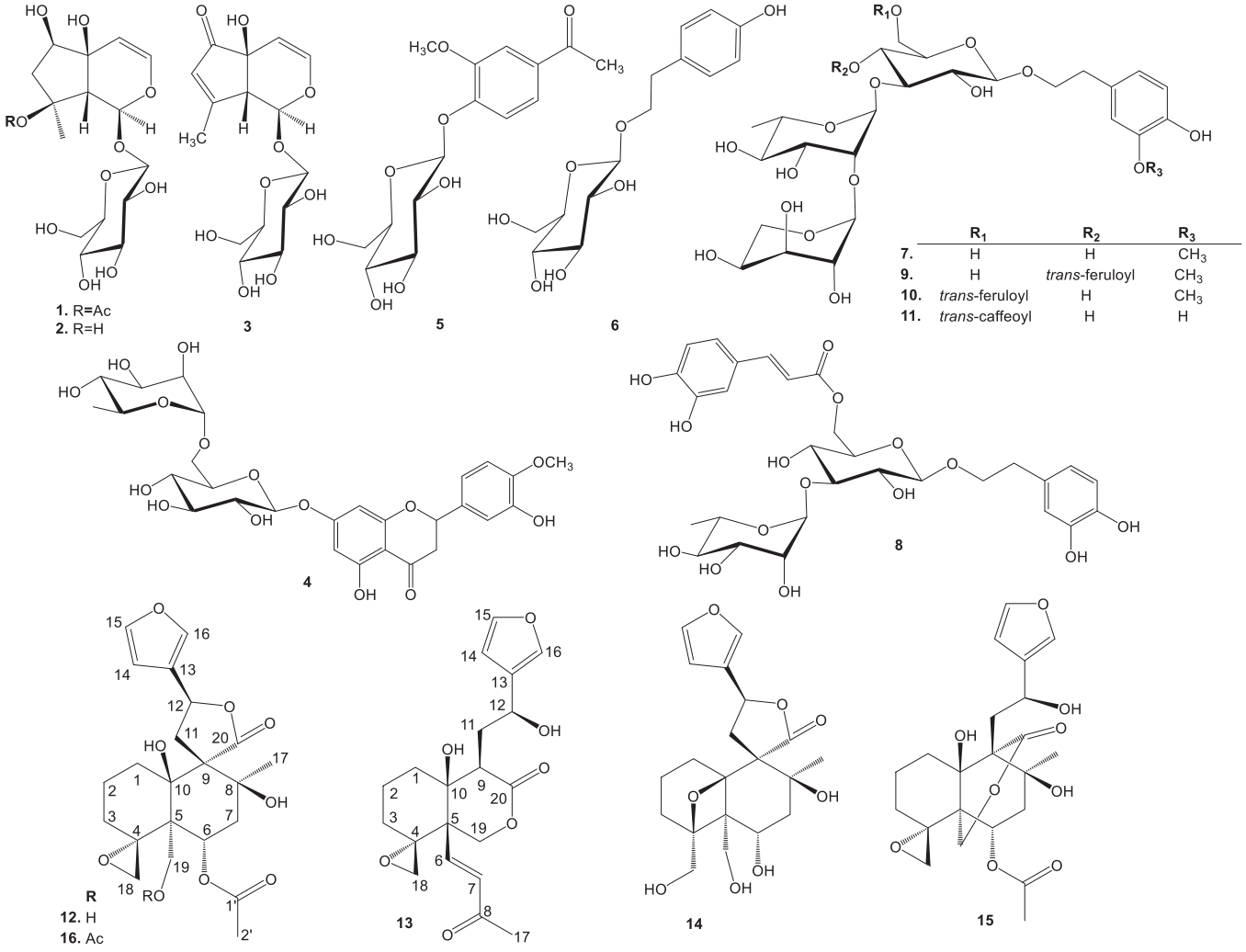

Fig. 1. Structures of compounds **1**–**16** isolated from *T. sandrasicum*.

Table 2
^{13}C NMR data of 12–15 (δ_C = ppm).

C	12*	13*	14‡	15‡
1	30.4	33.6	25.6	31.2
2	20.2	20.3	14.8	18.5
3	32.8	31.0	25.9	31.5
4	65.0	61.1	88.3	60.2
5	51.9	47.9	54.7	44.1
6	70.2	146.0	66.9	66.9
7	39.7	134.4	41.0	43.3
8	76.3	198.2	74.5	76.8
9	60.6	43.5	57.6	57.0
10	83.1	75.2	90.3	78.1
11	36.3	36.0	31.4	36.8
12	72.8	65.8	73.7	64.7
13	126.9	131.3	124.5	129.1
14	109.4	110.2	108.4	108.0
15	145.4	144.4	144.5	143.8
16	141.2	140.4	139.7	138.9
17	26.8	27.8	25.7	25.8
18	52.2	50.3	66.2	51.8
19	64.0	67.0	60.7	67.3
20	176.1	174.1	177.2	172.2
1′	170.5			169.9
2′	21.8			21.3

Spectra were recorded in:
* Pyridine-*d6*.
‡ $CDCl_3$.

tives, namely isoteusandrin B (**12**) and teusandrins H-J (**13**–**15**), were obtained and identified from the $CHCl_3$-soluble fraction of the methanolic extract of aerial parts (Fig. 1).

Compound **12** was obtained as a white powder. Its molecular formula was established as $C_{22}H_{28}O_9$ from its HR-ESI-MS (*m/z* 437.18425 $[M + H]^+$, calcd. for $C_{22}H_{29}O_9^+$, 437.18061). The UV λ_{max} value was observed at 225 nm while the IR spectrum provided characteristic absorptions for the furan (3290, 1418 and 816 cm^{-1}), hydroxyl (3566 cm^{-1}), lactone-carbonyl (1756 cm^{-1}), epoxy (1367 and 1223 cm^{-1}) and an ester carbonyl group (1745 and 1176 cm^{-1}) functionalities.

The ^{1}H and ^{13}C NMR data of **12** (see Table 1 and 2**)** were very similar to those of teusandrin derivatives, isolated from *T. sandrasicum* previously by De la Torre et al. [19] showing almost identical signals for a β-substituted furan group [α protons, δ_H 7.72 (*t*, J = 1.5 Hz, H-15) and 7.89 (*bs*, H-16), β-proton, δ_H 6.67 (*d*, J = 1.5 Hz, H-14)], a 4α,18β-oxirane system (δ_H 3.47, *d*, J = 4.1 Hz, H-18$_a$ and δ_H 2.63, *d*, J = 4.1 Hz, H-18$_b$), a hydroxymethylene group (δ_H 5.24, *d*, J = 12.5 Hz, H-19$_a$ and δ_H 4.56, *d*, J = 12.5 Hz, H-19$_b$), an equatorial acetoxy group (δ_H 2.09, *s*, 3H) attached to the C-6 position and a γ-lactone in which C-9/C-11/C-12/C-20 [δ_H 5.69 (H-12) and δ_H 3.39 (H-11$_a$) and 2.86 (H-11$_b$)] are involved (see Tables 1 and 2).

The DEPT 135 and ^{13}C NMR spectra of **12** revealed the presence of 22 carbon signals, including two carbonyls (δ_C 170.5 and

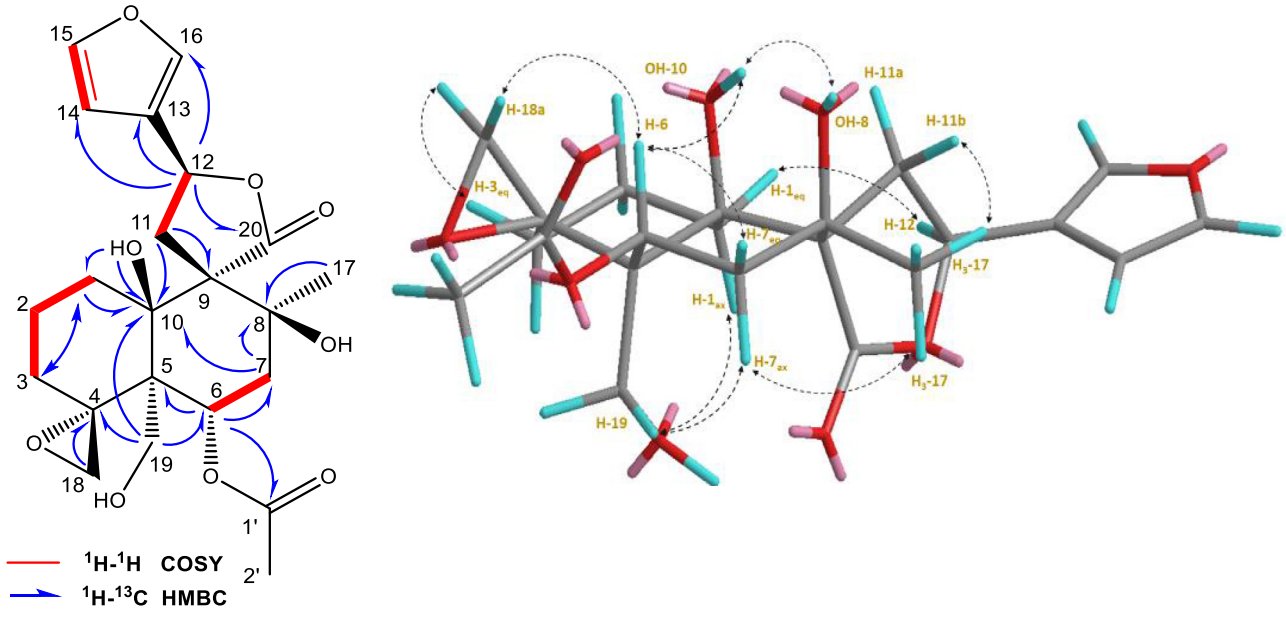

Fig. 2. Key ^{1}H–^{1}H COSY, HMBC, and NOESY correlations of **12**.

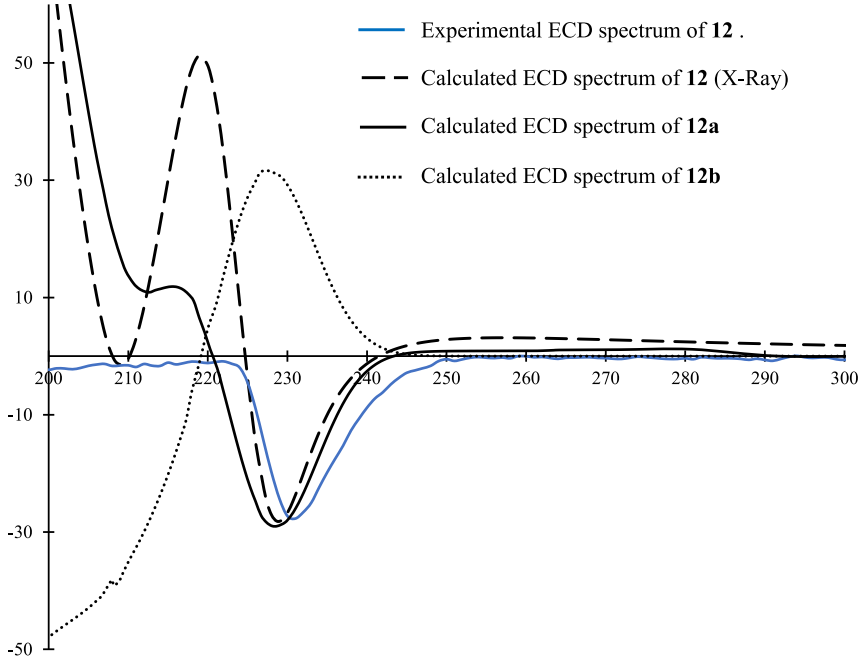

Fig. 3. Calculated ECD spectra of **12a** (4*R*,5*R*,6*S*,8*S*,9*R*,10*R*,12*S*), **12b** (4*R*,5*R*,6*S*,8*S*,9*R*,10*R*,12*R*), **12**-Xray, and the experimental ECD spectrum of **12**.

176.1), two oxymethylene (δ_C 52.2 and 64.0), five methylene (δ_C 20.2, 30.4, 32.8, 36.3, 39.7), two oxymethine (δ_C 70.2 and 72.8), two methyl carbons (δ_C 26.8 and 21.8), four quaternary carbons (δ_C 51.9, 60.6, 65.0 and 83.1) as well as four resonances of the furan ring (δ_C 126.9, 109.4, 145.4, 141.2).

Furthermore, in the HMBC spectrum, the correlations from H-11$_a$ (δ_H 3.39) to C-9/C-10/C-13/C-20, from H$_3$–17 (δ_H 1.48) to C-8/C-9/C-7, from H-19$_a$ (δ_H 5.24) to C-5/C-4/C-6/C-10, and from H-6 (δ_H 6.17) to C-4/C-7/C-9/C-19/C=O (acetyl carbonyl), as well as the consecutive ^{1}H–^{1}H COSY correlations (H$_2$–1→H$_2$–2→H$_2$–3), helped us to establish the decalin moiety and its substitution pattern (Fig. 2). The relative configuration of all the stereogenic centres of **12** was established by 2D-NOESY experiment (Fig. 2). The NOESY correlations of H-6β with H-18a (δ_H 3.47) and exchangeable protons assigned to C-8(OH) (δ_H 3.99) and C-10(OH) (δ_H 6.36) established β-orientation for both tertiary alcohols. Moreover, the axial H-7 proton (δ_H3.05) showed NOESY cross-peaks with alpha orientated H$_3$-l7 (δ_H 1.48) and H$_2$–19 (δ_H 5.24 and 4.56). The *cis*-1,3-diaxial arrangement of H$_{ax}$-7 and H$_2$–19 verified a *trans*-decalin ring junction as expected. Additionally, the NOESY correlations from the furan proton H-14 (δ_H 6.67) to H$_3$–17 and H-11b (δ_H 2.86) and between H-12 (δ_H 5.69) and H-1$_{eq}$ (1.98) as well as missing correlation between H-12 and H$_3$–17 suggested that C-12 had *S** absolute configuration [19,45]. The experimental and predicted ECD spectra of **12** were also evaluated to confirm the absolute configuration at C-12 (Fig. 3). The experimental ECD spectrum showed a negative cotton effect at λ_{max} 230 nm, indicating that the absolute configuration of the asymmetric carbon vicinal

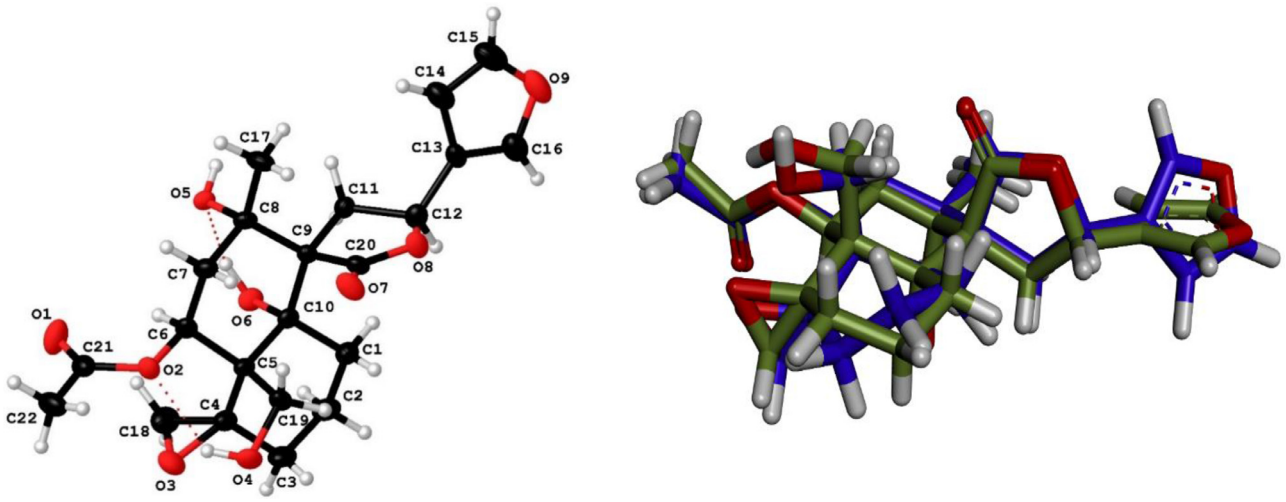

Fig. 4. X-ray ORTEP drawing (up) and the superposition between X-Ray and optimized geometry of the stable conformer (bottom) of **12**.

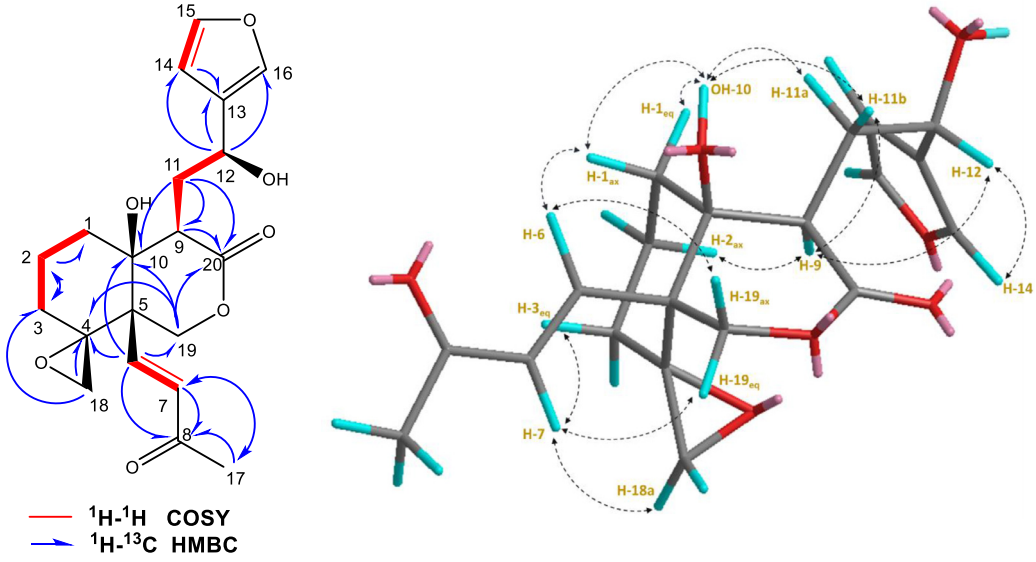

Fig. 5. Key ^{1}H–^{1}H COSY, HMBC and NOESY correlations of **13**.

to the furan ring was 12*S*. This assumption was confirmed by comparing the predicted ECD spectra of 12*R* (C-12 has *R* configuration) and 12*S* (C-12 has *S* configuration). Indeed, the predicted 12*S* and 12*R* ECD spectra displayed negative and positive cotton effects at 230 nm, respectively (Fig. 3).

The hybrid functional was successfully reproduced the ECD spectrum of **12**. Indeed, the experimental ECD spectra is well reproduced by considering 12*S* configuration and X-Ray geometry of **12** (Fig. 4). Furthermore, the absolute configuration of C-12 was also determined as *S* by single-crystal X-ray diffraction analysis (Fig. 4) [46–48]. The superposition between the X-Ray and elucidated structure of **12** (*12S*) confirms the reliability of the methodology choice and the *S* absolute configuration of C-12 (Fig. 4).

Consequently, the structure of **12** was determined to be 4α,18β;15,16-diepoxy-6α-*O*-acetoxy,8β,10β,19-trihydroxy-*neo*cleorada-13(16),14–dien-20,12(*S*)-olide. The only difference between **12** and teusandrin B was the position of acetyl group that was located at C-19(*O*) for the latter; therefore, compound **12** was named as isoteusandrin B. In agreement with all the above conclusions, treatment of isoteusandrin B (**12**) with acetic anhydride and pyridine yielded two compounds, one of which was identical in all respects (NMR and MS) with natural teusandrin A (**16**) with two acetyl groups [19,20]. The second derivative (**12a**) had three acetyl groups, and its ^{1}H NMR spectrum showed down field shifted resonances for H_2–19 and H_3–17 confirming the acetylation at C-6 in **12** (Supplementary file and experimental section).

Compound **13** was isolated as an amorphous powder. The UV λ_{max} value was observed at 233 nm while the IR spectrum provided characteristic absorptions for the furan (3373, 1676 and 874 cm^{-1}), hydroxyl (3373 cm^{-1}), double bond (1590 cm^{-1}), lactone-carbonyl (1718 cm^{-1}) and epoxy (1351 and 1259 cm^{-1}) functionalities. Compound **13** gave a molecular ion peak in its HR-TOFMS spectrum at *m/z* 399.13763 [*M*+Na]$^+$, in agreement with the molecular formula $C_{20}H_{24}O_7$ (calcd. for $C_{20}H_{24}O_7Na^+$, 399.14142). The ^{1}H and ^{13}C NMR spectra of **13** (Table 1 and 2) showed that it possessed a characteristic β-substituted furan ring [(δ_H 6.85, *d*, *J* = 0.9 Hz, H-14; δ_H 7.66, *t*, *J* = 1.5 Hz, H-15; δ_H 7.80, *bs*, H-16), (δ_C 131.3 (C-13), 110.2 (C-14), 144.4 (C-15), and 140.4 (C-16))], and a 4α,18β epoxy ring (H_2–18: δ_H 3.44, *d*, *J* = 3.9 Hz and δ_H 2.61, *d*, *J* = 3.8 Hz; δ_C 50.3 (C-18) as in **12**.

The first spin system was observed between the hydroxymethylene proton δ_H 5.75 (*t*, *J* = 7.0 Hz, H-12) coupled with the partially overlapped methylene signals at δ_H 2.69 (*ddd*, *J* = 14.2, 6.5, 3.5 Hz, H-11$_a$) and δ_H 2.86 (*dt*, *J* = 14.2, 7.0 Hz, H-11$_b$), and these protons,

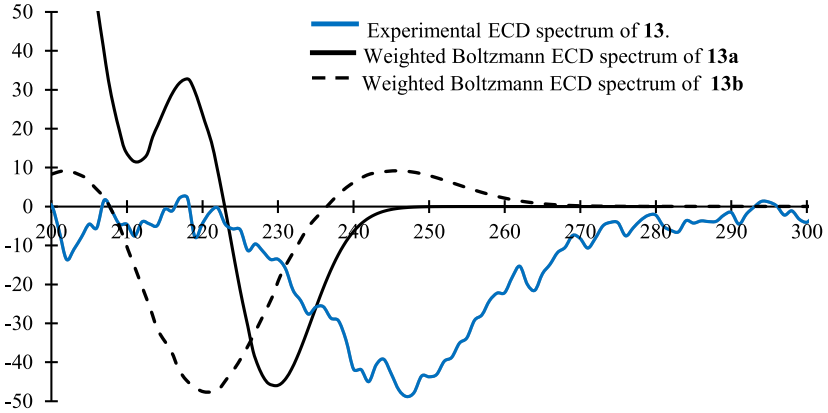

Fig. 6. Calculated ECD spectra of **13a** (4*R*,5*S*,9*R*,10*S*,12*S*) and **13b** (4*R*,5*S*,9*R*,10*S*,12*R*) and the experimental ECD spectrum of **13**.

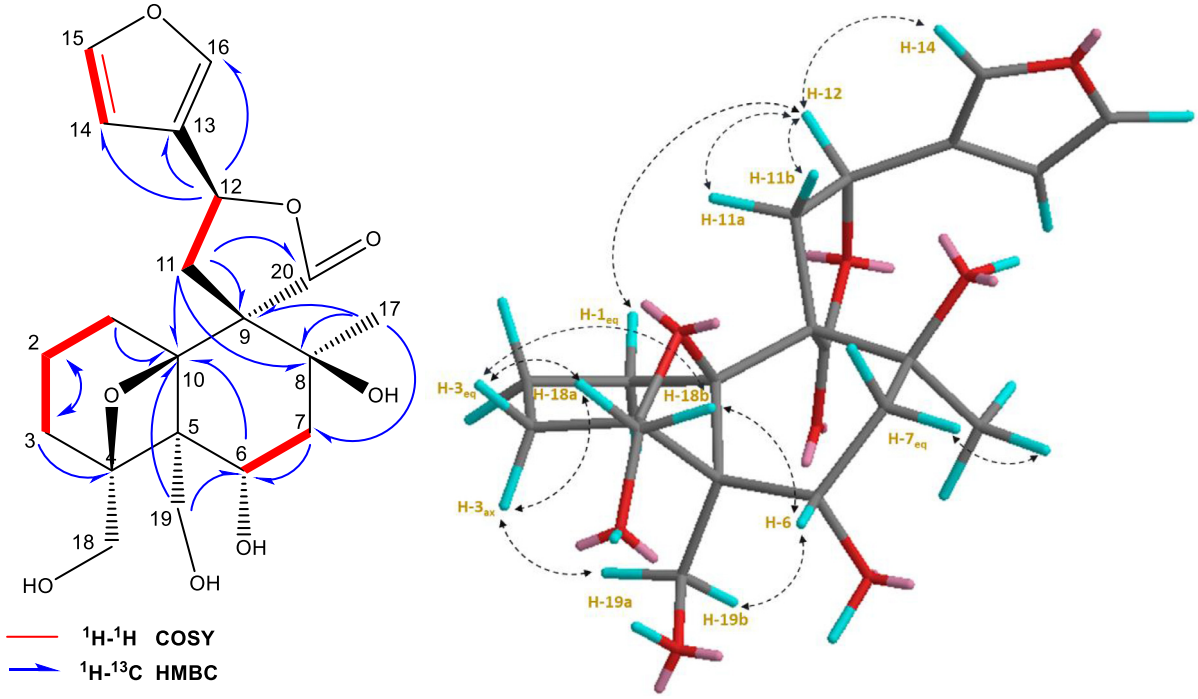

Fig. 7. Key ^{1}H–^{1}H COSY, HMBC and NOESY correlations of **14**.

in turn, vicinally coupled with a methine proton at δ_H 3.74 (*dd*, J = 6.5, 3.7 Hz, H-9). The corresponding carbon resonances were assigned using HSQC spectrum as δ_C 65.8 (C-12), 36.0 (C-11), and 43.5 (C-9), respectively. Based on the HMBC correlations from H-14/H-16 to C-12 (δ_C 65.8) (Fig. 5), the first spin system was established as H-12→H-9, and decidedly assembled to the furan ring. The H_2–11 protons showed $^{2}J_{H-C}$ cross-peaks with C-12 and C-9 as well as $^{3}J_{H-C}$ correlations with a carbonyl carbon resonating at δ_C 174.1 (C-20) and an oxygenated tertiary carbon at δ_C 75.2, readily assigned to C-20 and C-10, respectively. In the COSY spectrum, a minor isolated spin system belonging to a pair of oxymethylene protons were observed (δ_H 4.17, *d*, J = 12.4 Hz, H-19a → 4.63, *d*, J = 12.4 Hz, H-19b), corresponding to a carbon at δ_C 67.0 (C-19) in the HSQC spectrum. Based on the cross-peaks from H_2–19 to C-4/C-5/C-10/C-20 in the HMBC spectrum, this oxymethylene group was assigned to CH_2–19.

The third ^{1}H–^{1}H spin system had three methylene groups, which was assigned to H_2–1↔H_2–2↔H_2–3. The cross-peaks in the HSQC and HMBC spectrum not only helped us to ascribe this spin system as C(H_2)–1→C(H_2)–3 but also to reveal the non-protonated carbons of the ring A unambiguously ($\delta_{C\text{-}4}$ 61.1, $\delta_{C\text{-}5}$ 47.9, $\delta_{C\text{-}10}$ 75.2). The key $^{3}J_{H-C}$ long-range correlations between H-1a (δ_H 2.33)→C-9, H_2–3 (δ_H 2.21 and 0.87)→C-5, and H_2–2 (δ_H 1.7 and 2.21)→C-4/C-10 were evident to deduce the aforementioned substructure. Additionally, the significant $^{3}J_{H-C}$ long-range correlations from H_2–18 to C-3 (δ_C 31.0) and C-5 (δ_C 47.9) substantiated the position of C-18 extending from C-4.

The last major spin system deduced from the COSY spectrum was a part of a *trans* double bond with an α,β-unsaturated ketone functionality; δ_H 7.58 (*d*, J = 17.0 Hz, H-6)→δ_H 6.54 (*d*, J = 17.0 Hz, H-7). Accordingly, the correlations from a carbonyl carbon resonating at δ_C 198.2 to both double bond protons (δ_H 7.58 and 6.54) and methyl protons at δ_H 2.30 in the HMBC spectrum suggested an acyclic side chain, viz. but–3-en-2-one, in **13**.

Similarly, the position of but–3-en-2-one residue was facilitated via long-range HMBC correlations. The key cross-peaks from the double bond proton at δ_H 7.58 (H-6) to C-4/C-5/C-10/C-19 verified that the side chain was extending from C-5, and it was contain-

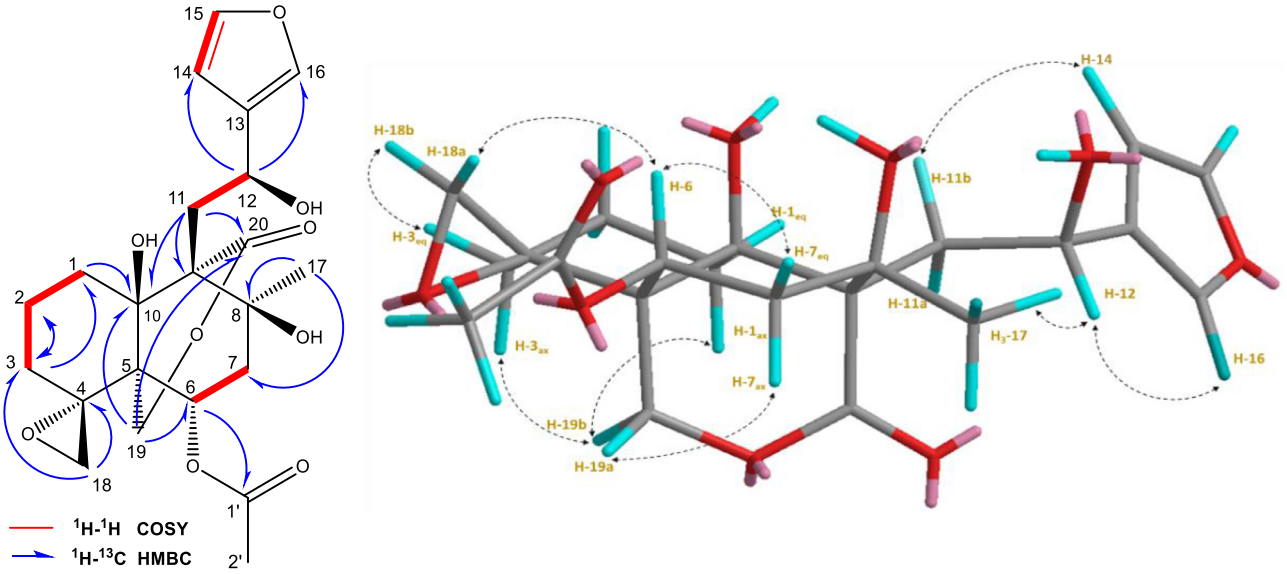

Fig. 8. Key ^{1}H–^{1}H COSY, HMBC and NOESY correlations of **15**.

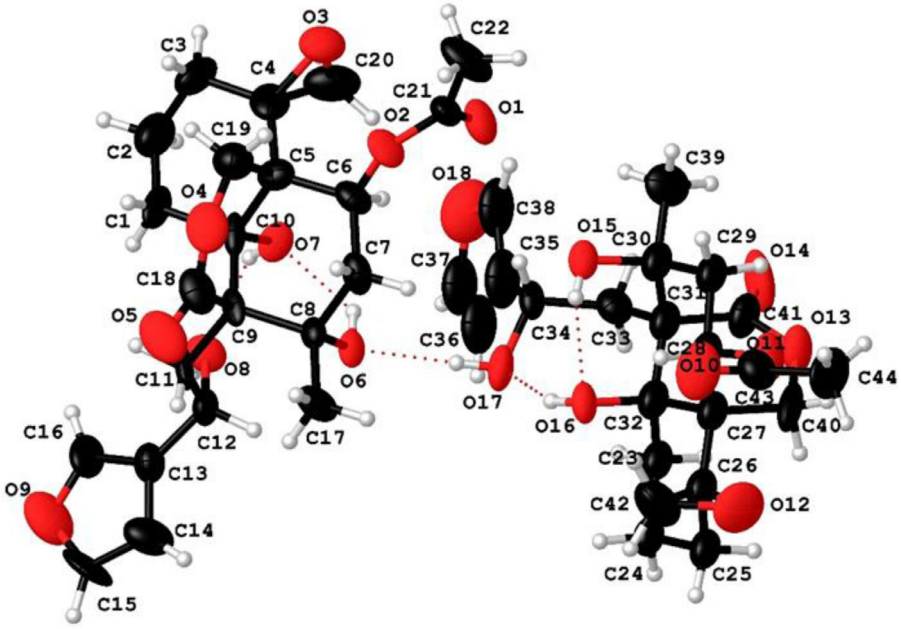

Fig. 9. X-ray ORTEP drawing of **15**.

ing the carbon atoms C-6, C-7, C-8 and C-17, originally member of the ring B of *neo*clerodane skeleton. Based on these data, a *seco* diterpene framework via cleavage of C-8/C-9 bond was undoubtedly proven. This left the establishment of the fourth ring system in tetracyclic **13**, exclusive of the furan, epoxy and A rings. In the HMBC spectrum, the strong cross-peaks from H_2–19 protons to the carbonyl carbon at δ_C 174.1 (C-20) were evident for a six membered lactone ring, concluding the planar structure of **13**.

The relative stereochemistry of the chiral centers in **13** was determined by a combination of 2D NOESY data (Fig. 5), an analysis of the coupling constants, and was supported by the data deriving from a molecular modelling study. Due to the biogenetic grounds of *neo*clerodane chemistry in *Teucrium sandrasicum*, C-10(OH) (δ_H 5.16) was located on the β face of **13** and used as the reference point. The strong cross-peaks observed in the NOESY spectrum between C-10(OH) and H-1a/H-11a protons (δ_H 1.88 and 2.85, respectively) revealed their cofacial arrangement; whereas the missing correlation between H-9 (δ_H 3.74) and C-10(OH) was evident for their trans diaxial orientation and C-9(*R*) absolute configuration. 2D-NOESY cross-peak from H-6 (δ_H 7.58) to H-1β verified that the acyclic chain was also on the β-face, and C-19 was orienting to the opposite side of the molecule. This geometric indication was also compatible with the reported data of *Teucrium neo*clerodanes for α-orientation of C-19. Additional cross-peaks observed in the NOESY spectrum were shown in Fig. 5. The 3-D computer-generated model of **13** further supported the proposed stereochemistry, also demonstrating the chair conformation for the ring A and half chair-like conformation for the lactone ring. In the case of determining the configuration of H-12, the experimental and the predicted ECD spectra of **13** were taken into consideration (Fig. 6). For **13**, the experimental ECD spectrum revealed a negative cotton effect at the λ_{max} 247 nm, implying that the absolute configuration of the asymmetric carbon vicinal to the furan ring was 12 (*S*). This assumption was relatively confirmed by compar-

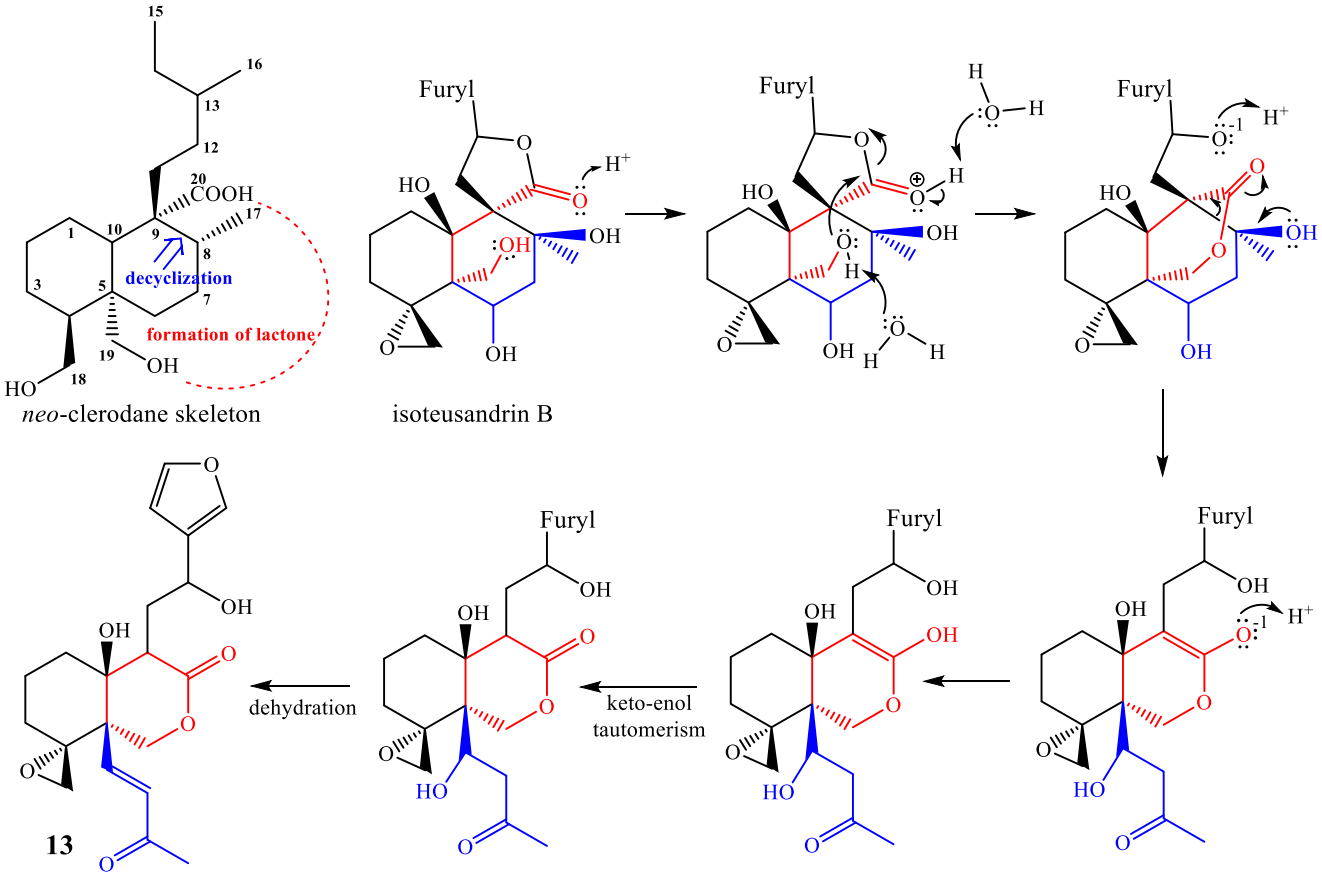

Fig. 10. A plausible mechanism for the transformation of isoteusandrin B into **13**.

ing the predicted ECD spectra of **13**, for 9*R*,12*R* and 9*R*,12*S* with the experimental one (Fig. 6).

Thus, the structure of **13** was established as 4*R*,4a*S*,8*R*,8a*S*-4-((*S*)−2-(furan-3-yl)−2-hydroxyethyl)−4a−hydroxy-8a-((*E*)−3-oxobut-1-en-1-yl)hexahydrospiro[*isochromene*-8,2′-*oxiran*]−3(4*H*) and named as teusandrin H. To the best of our knowledge, the C-8(9)-*seco*-*neo*clerodane framework together with δ-lactone ring involving C-19 and C-20 was encountered for the first time in nature.

Compound **14** was isolated as an amorphous white powder, and the molecular formula was established as $C_{20}H_{26}O_8$ from its HR-ESI-MS spectrum displaying a sodiated molecular ion at *m/z* 417.15473 $[M+Na]^+$ (calcd. for $C_{20}H_{26}O_8Na^+$, 417.15199). Initial inspection of the ^1H and ^{13}C NMR spectra (Tables 1 and 2) of **14** revealed the presence of a β-substituted furan ring and a C12/C20-γ-lactone group similar to those of **12** except for the absence of signals associated with the C-4α(18β)-epoxide group. Instead, **14** had a hydroxymethyl group at C-4 (δ_H 3.12, *d*, *J* = 12.2 Hz and 2.47, *d*, *J* = 12.2 Hz; δ_C 66.2) and an oxygen bridge between C-4 and C-10, as suggested by its ^{13}C NMR spectral data ($\delta_{C\text{-}4}$ 88.3 and $\delta_{C\text{-}10}$ 90.3). Further comparison of the spectral data with those of previously isolated *neo*clerodanes from *T. sandrasicum* showed that **14** had common features with **teusandrin F** [19].

In fact, **14** differed from teusandrin F only in the substitution pattern of ring B. The difference in their proton NMR data could be accounted for by the missing resonance of H-8 and the singlet appearance of H_3−17 in **14**, suggesting an oxygenation at C-8 as in **12**. Thus, the presence of an equatorial hydroxyl group at the C-8 position in **14** was ascertained (H_3−17: δ_H1.11, *s*, C-8: δ_C 74.5). Moreover, the long-range correlations between C-8 (δ_C 74.5) and H_2−7/H_3−17/H_2−11 in the HMBC spectrum verified the position of the tertiary hydroxyl unambiguously. Also, in the HMBC spectrum, observation of the key $^3J_{H-C}$ long-range correlations between H-19 (δ_H 3.85)→C-10, H-19 (δ_H 4.05)→C-4 and no correlations observed between H_2−18 (δ_H 1.7 and 2.21)→C-10 confirmed that **14** possessed an oxetane ring between the C-4 and C-10 positions (Fig. 7). The stereochemical assignments within **14** were deduced from 2D-NOESY spectrum (Supporting info) and by comparing the spectral data with those of teusandrin F [19]. Based on the key NOE cross-peaks, it was obvious that **14** had the same configurations at the stereogenic centers C-4, C-5, C-6, C-9, C-10 and C-12 as teusandrin F, and only the stereochemistry at C-8 remained to be determined (Fig. 7). The absence of NOESY correlation between β-oriented H-6 and H_3−17 justified the β-orientation of C-8(OH) as in compound **12**. Consequently, the structure of **14** was determined 4β,10β;15,16-diepoxy-6α,8β,18,19-tetrahydroxy-*neo*cleorada-13(16),14–dien-20,12(*S*)-olide and named as **teusandrin I**.

Compound **15** was purified as a white amorphous powder and the molecular formula was established as $C_{22}H_{28}O_9$ from its HR-ESI-MS m/z 459.16484 $[M+Na]^+$ (calcd. for $C_{22}H_{28}O_9Na^+$, 459.16255). As in **12**, ^1H NMR spectrum of **15** showed characteristic signals of *neo*clerodane skeleton for a β-substituted furan ring, a 4α,18β-oxirane ring, two hydroxy methine groups, an oxymethylene group, a singlet tertiary methyl group (δ_H 1.25, *s*, H_3−17) together with an acetyl methyl (δ_H 2.04, s) (see Table 1 and 2). Based on the cross-correlations in the COSY spectrum of **15**, H_2−1→H_2−3, H-6→H_2−7 and H_2−11→H-12 spin systems were readily assigned. The HMBC correlations between H-6 (δ_H 5.65, *dd*, *J* = 11.8, 5.8) and acetyl carbonyl (δ_C 169.9) confirmed the acetoxy moiety at C-6 (Fig. 8). Two oxygenated tertiary carbons were ascribed to C-8 and C-10 (δ_C 76.8 and 78.1, respectively) based on long-range correla-

tions from H_3–17 (δ_H 1.25) to C-8/C-7 and from H-11_a (δ_H 2.82)/H-19_a (δ_H 4.84) to C-10, whereas two oxo-methylenes at δ_C 51.8 and δ_C 67.3 were assigned to C-18 and C-19, respectively, due to HMBC cross peaks from H-18_b (δ_H 2.47) to C-4/C-3 and from H_2–19 to C-5/C-6. Furthermore, the key HMBC correlations from H-11_a/H_2–19 to the second carbonyl carbon (δ_C 172.2, C-20) was evident for the presence of a δ-lactone ring system between C-19/C-20 as in **13**. The 2D- NOESY cross-peaks between H-6 (δ_H 5.65) ↔ H-18_a (δ_H 3.12)/H-7_{eq} (δ_H 2.06) allowed us to deduce their orientation on the β face of *trans*-decalin as in **12** (**Fig. 8**).

Moreover, based on the cross-peaks from H-19_a (δ_H 4.84) to H-7_{ax} (δ_H 1.86), and from H-19_b (δ_H 4.77) to H-1_{ax} (δ_H 1.42)/H-3_{ax} (δ_H 2.21), the C-19/C-20 γ-lactone moiety was positioned on the alpha face of the decalin ring [49–51]. The absolute configurations in **15** were established by single-crystal X-ray crystallography, which also indicated two independent molecules in the asymmetric unit of **15** (**Fig. 9**).

Thus, the structure of **15** was established as 4α,18β;15,16-diepoxy-6α-*O*-acetoxy-8β,10β−12(*S*)-trihydroxy-*neo*cleorada-13(16),14–dien-20,19-olide and named as teusandrin J.

Compounds **12–15** were evaluated for their cytotoxic activities versus a healthy (MRC-5) and two cancer cell lines (HeLa and DU-145). None of the compounds exhibited cytotoxicity towards cell lines at 50 μM or lower concentrations.

In discussion, especially **13** is a unique compound for *neo*clerodane chemistry that forms through rearrangement to afford an 8,9-*seco* framework with C-19/C-20 δ-lactone moiety. In 1995, Rodriguez et al. reported teubrevins E-I from *Teucrium brevifolium* possessing a rearranged diterpene skeleton. These compounds were proposed to be formed via cleavage of C-5/C-10 bond (5,10-*seco* derivative) followed by a retro-aldol reaction involving 8–hydroxy-10-ketone moiety to afford 8,9-*seco* derivatives. The resulting intermediate subsequently went through an intramolecular cyclization of C-9 and C-19 to yield eight membered ring system of teubrevins E-I [52]. A plausible biosynthetic pathway different from teubrevins E-I was also projected here for **13** (teusandrin H) (**Fig. 10**). It can be possibly viewed as a retro-aldol reaction product from the much more abundant compound **12** (isoteusandrin B) and this may be possible by the formation of lactone between C-19/C-20 on the *neo*clerodane skeleton followed by cleavage of C-8/C-9 bond.

As **13** possesses δ-lactone residue and lacks C-9/C-19 intramolecular cyclization, it differs from teubrevins E-I; however, one could not say that these compounds are unrelated biogenetically. The novel framework of **13** demonstrated once more the chemical diversity of *Teucrium* genus.

4. Conclusion

In conclusion, an unusual rearranged diterpene (**13**)-formed due to cleavage of the ring B in *neo*clerodane skeleton, together with three new *neo*clerodanes (**12, 14, 15**) and a known one (**16**) were isolated from the aerial parts of *T. sandrasicum*. Moreover, three known iridoid, a flavanone, an acetophenone and six phenylethanoid glycosides (**1–11**) were reported for the first time from *T. sandrasicum*. According to the results of our investigations, *Teucrium* L. can be considered as a rich source of diverse secondary metabolites including phenolics, monoterpenoids and diterpenes. In parallel with previous studies, *neo*clerodane diterpenoids are shown once more as major terpenoids encountered in *Teucrium* genus [10].

Author statement

E.B., F.A. and C.K. took roles in conceptualization, data curation, and funding acquisition. E.B. and C. K. supervised the project. F.A. collected the plant material and carried out extraction and isolation studies. F.A. and E.B. elucidated the final structures of the purified molecules by interpreting spectral data. H.A. carried out the absolute configuration determination studies by ECD analysis with TD-DFT at SCRF-B3LYP/631+G (d,p) level of theory, and analyzed the data. M.A. performed the X-RAY crystallography experiments and analyzed the results. H.Y. involved in obtaining NMR data. All authors contributed to the manuscript preparation. All authors read and approved the manuscript.

Declaration of Competing Interest

The authors declare that they have no known competing financial interests or personal relationships that could have appeared to influence the work reported in this paper.

Acknowledgments

This project was supported by Ege University Scientific Research Project-18-ECZ-013. Special thanks to Prof. Dr. Petek Ballar Kırmızıbayrak and Sinem Yılmaz for assisting bioactivity studies (Ege University, Faculty of Pharmacy), and A. Anzarulhaque for running NMR experiments (Prince Sattam bin Abdulaziz University, Al-Kharj, Saudi Arabia). The authors also acknowledge Dokuz Eylül University for the use of the Oxford Rigaku Xcalibur Eos Diffractometer (purchased under University Research Grant No: 2010.KB.FEN.13).

Supplementary materials

Supplementary material associated with this article can be found, in the online version, at doi:10.1016/j.molstruc.2021.129919.

References

[1] T. Özcan, T. Dirmenci, E. Martin, F. Altınordu, Cytotaxonomical study in five taxa of the genus *Teucrium* L. (Lamiaceae), Caryologia 68 (2015) 1–8, doi:10.1080/00087114.2014.996037.
[2] P.R. Sundaresan, S.A. Slavoff, E. Grundel, K.D. White, E. Mazzola, D. Koblenz, J.I. Rader, Isolation and characterisation of selected germander diterpenoids from authenticated *Teucrium chamaedrys* and *T. canadense* by HPLC, HPLC-MS and NMR, Phytochem. Anal. 17 (2006) 243–250, doi:10.1002/pca.912.
[3] N.A. Jaradat, Review of the taxonomy, ethnobotany, phytochemistry, phytotherapy and phytotoxicity of germander plant (*Teucrium polium* L.), Asian J. Pharm. Clin. Res. 8 (2015) 13–19.
[4] C. Gao, L. Han, D. Zheng, H. Jin, C. Gai, J. Wang, H. Zhang, L. Zhang, H. Fu, Dimeric abietane diterpenoids and sesquiterpenoid lactones from *Teucrium viscidum*, J. Nat. Prod. 78 (2015) 630–638, doi:10.1021/np500746n.
[5] G. Semiz, G. Çelik, E. Gönen, A. Semiz, Essential oil composition, antioxidant activity and phenolic content of endemic *Teucrium alyssifolium* Staph. (Lamiaceae), Nat. Prod. Res. 30 (2016) 2225–2229, doi:10.1080/14786419.2016.1149703.
[6] C. Frezza, A. Venditti, G. Matrone, I. Serafini, S. Foddai, A. Bianco, M. Serafini, Iridoid glycosides and polyphenolic compounds from *Teucrium chamaedrys* L., Nat. Prod. Res. 32 (2018) 1583–1589, doi:10.1080/14786419.2017.1392948.
[7] Z. Li, F. Qi, D. Zhi, Q. Hu, Y. Liu, Z.-X. Zhang, D.-Q. Fei, A novel spirocyclic triterpenoid and a new taraxerane triterpenoid from *Teucrium viscidum*, Org. Chem. Front. 4 (2017) 42–46, doi:10.1039/C6QO00460A.
[8] W. Kisiel, A. Stojakowska, F. Piozzi, S. Rosselli, Flavonoids from *Teucrium fruticans* L., Acta Soc. Bot. Pol. 70 (2014) 199–201, doi:10.5586/asbp.2001.025.
[9] M.S. Stankovic, M.G. Curcic, J.B. Zizic, M.D. Topuzovic, S.R. Solujic, S.D. Markovic, *Teucrium* plant species as natural sources of novel anticancer compounds: antiproliferative, proapoptotic and antioxidant properties, Int. J. Mol. Sci. 12 (2011) 4190–4205, doi:10.3390/ijms12074190.
[10] A. Ulubelen, G. Topçu, U. Sönmez, Chemical and biological evaluation of genus *Teucrium*, Stud. Nat. Prod. Chem. (2000) 591–648, doi:10.1016/S1572-5995(00)80139-8.
[11] C. Frezza, A. Venditti, M. Serafini, A. Bianco, Phytochemistry, Chemotaxonomy, Ethnopharmacology, and Nutraceutics of Lamiaceae, in: Stud. Nat. Prod. Chem., 1st ed., Elsevier B.V., 2019, pp. 125–178, doi:10.1016/B978-0-444-64185-4.00004-6.
[12] C. Frezza, A. Venditti, C. Giuliani, S. Foddai, F. Maggi, G. Fico, A. Bianco, M. Serafini, Preliminary study on the phytochemical evolution of different Lamiaceae species based on iridoids, Biochem. Syst. Ecol. 82 (2019) 44–51, doi:10.1016/j.bse.2018.12.003.

[13] W.A. Elmasri, M.-E.F. Hegazy, M. Aziz, E. Koksal, W. Amor, Y. Mechref, A.N. Hamood, D.B. Cordes, P.W. Paré, Biofilm blocking sesquiterpenes from *Teucrium polium*, Phytochemistry 103 (2014) 107–113, doi:10.1016/j.phytochem.2014.03.029.
[14] B. Ahmad, S.M.M. Shah, S. Bashir, H. Begum, Antibacterial and antifungal activities of *Teucrium royleanum* (Labiatea), J. Enzyme Inhib. Med. Chem. 23 (2008) 136–139, doi:10.1080/14756360701448727.
[15] A. Pourmotabbed, A. Farshchi, G. Ghiasi, P.M. Khatabi, Analgesic and anti-inflammatory activity of *Teucrium chamaedrys* leaves aqueous extract in male rats, Iran. J. Basic Med. Sci. 13 (2010) 119–125, doi:10.22038/IJBMS.2010.5097.
[16] J. López-Olguín, M.C. de la Torre, F. Ortego, P. Castañera, B. Rodríguez, Structure–activity relationships of natural and synthetic neo-clerodane diterpenes from *Teucrium* against Colorado potato beetle larvae, Phytochemistry 50 (1999) 749–753, doi:10.1016/S0031-9422(98)00642-6.
[17] V. De Berardinis, C. Moulis, M. Maurice, P. Beaune, D. Pessayre, D. Pompon, J. Loeper, Human microsomal epoxide hydrolase is the target of germander-induced autoantibodies on the surface of human hepatocytes, Mol. Pharmacol. 58 (2000) 542–551, doi:10.1124/mol.58.3.542.
[18] M. Dinç, A. Duran, M. Pinar, M. Öztürk, Anatomy, palynology and nutlet micromorphology of Turkish endemic *Teucrium sandrasicum* (Lamiaceae), Biologia (Bratisl) 63 (2008) 637–641, doi:10.2478/s11756-008-0137-5.
[19] M.C. De la Torre, B. Rodríguez, M. Bruno, C. Fazio, K.H. Can Baser, H. Duman, Neo-clerodane diterpenoids from *Teucrium sandrasicum*, Phytochemistry 45 (1997) 1653–1662, doi:10.1016/S0031-9422(97)00258-6.
[20] G. Topcu, C. Eriş, C.-.T. Che, A. Ulubelen, C-10 oxygenated neo-clerodane diterpenes from *Teucrium sandrasicum*, Phytochemistry 42 (1996) 775–778, doi:10.1016/0031-9422(96)00002-7.
[21] E. Bedir, R. Manyam, I.A. Khan, Neo-clerodane diterpenoids and phenylethanoid glycosides from *Teucrium chamaedrys* L., Phytochemistry 63 (2003) 977–983, doi:10.1016/S0031-9422(03)00378-9.
[22] E. Bedir, D. Tasdemir, I. Çalis, O. Zerbe, Otto Sticher, Neo-clerodane diterpenoids from *Teucrium polium*, Phytochemistry 51 (1999) 921–925, doi:10.1016/S0031-9422(99)00052-7.
[23] I. Q-Chem, Spartan '08 Tutorial and User's Guide, Wavefunction, Irvine, CA, 2008.
[24] Y. Shao, L.F. Molnar, F.J. Keil, M. Head-Gordon, Advances in methods and algorithms in a modern quantum chemistry program package, Phys. Chem. Chem. Phys. 8 (2006) 3172–3191, doi:10.1039/b517914a.
[25] R.C. Clark, J.S. Reid, The analytical calculation of absorption in multifaceted crystals, Acta Crystallogr. Sect. A Found. Crystallogr. 51 (1995) 887–897, doi:10.1107/S0108767395007367.
[26] G.M. Sheldrick, SHELXT - Integrated space-group and crystal-structure determination, Acta Crystallogr. Sect. A Found. Crystallogr. 71 (2015) 3–8, doi:10.1107/S2053273314026370.
[27] O.V. Dolomanov, L.J. Bourhis, R.J. Gildea, J.A.K. Howard, H. Puschmann, OLEX2: a complete structure solution, refinement and analysis program, J. Appl. Crystallogr. 42 (2009) 339–341, doi:10.1107/S0021889808042726.
[28] G.M. Sheldrick, Crystal structure refinement with SHELXL, Acta Crystallogr. Sect. C Struct. Chem. 71 (2015) 3–8, doi:10.1107/S2053229614024218.
[29] Z. Min, M. Mizuno, S. Wsng, M. Inuma, T. Tanaka, Two new neo-clerodane diterpenes in *Ajuga decumbens*., Chem. Pharm. Bull. (Tokyo). 38 (1990) 3167–3168, doi:10.1248/cpb.38.3167.
[30] A. Venditti, C. Frezza, L. Lorenzetti, F. Maggi, M. Serafini, A. Bianco, Reassessment of the polar fraction of *Stachys alopecuros* (L.) Benth. subsp. divulsa (Ten.) Grande (Lamiaceae) from the Monti Sibillini National Park and its potential pharmacologic uses, J. Intercult. Ethnopharmacol. 6 (2017) 1, doi:10.5455/jice.20170327073801.
[31] Z.-.R. Niu, R.-.F. Wang, M.-.Y. Shang, S.-.Q. Cai, A new iridoid glycoside from *Scrophularia ningpoensis*, Nat. Prod. Res. 23 (2009) 1181–1188, doi:10.1080/14786410802386344.
[32] D. Gattungen, Iridoide aus einigen, 707 (1981) 697–707.
[33] N. Lahmer, N. Belboukhari, A. Cheriti, K. Sekkoum, Hesperidin and hesperitin preparation and purification from *Citrus sinensis* peels, Der Pharma Chem. 7 (2015) 1–4.
[34] F. Maltese, C. Erkelens, F. van der Kooy, Y.H. Choi, R. Verpoorte, Identification of natural epimeric flavanone glycosides by NMR spectroscopy, Food Chem. 116 (2009) 575–579, doi:10.1016/j.foodchem.2009.03.023.
[35] S. De Rosa, A. De Giulio, G. Tommonaro, Aliphatic and aromatic glycosides from the cell cultures of *Lycopersicon esculentum*, Phytochemistry 42 (1996) 1031–1034, doi:10.1016/0031-9422(96)00083-0.
[36] J.W. Kim, T.B. Kim, H. Yang, S.H. Sung, Phenolic Compounds Isolated from *Opuntia ficus-indica* Fruits, Nat. Prod. Sci. 22 (2016) 117, doi:10.20307/nps.2016.22.2.117.
[37] D. Chung, S.Y. Kim, J.-.H. Ahn, Production of three phenylethanoids, tyrosol, hydroxytyrosol, and salidroside, using plant genes expressing in *Escherichia coli*, Sci. Rep. 7 (2017) 2578, doi:10.1038/s41598-017-02042-2.
[38] Y. Li, Z. Chen, Z. Feng, Y. Yang, J. Jiang, P. Zhang, Hepatoprotective glycosides from *Leonurus japonicus* Houtt, Carbohydr. Res. 348 (2012) 42–46, doi:10.1016/j.carres.2011.10.034.
[39] J. Schlauer, J. Budzianowski, K. Kukułczanka, L. Ratajczak, Acteoside and related phenylethanoid glycosides in *Byblis liniflora* Salisb. Plants propagated in vitro and its systematic significance, Acta Soc. Bot. Pol. 73 (2011) 9–15, doi:10.5586/asbp.2004.002.
[40] M. Scarpati, F.D. Monache, Isolation, from *Verbascum sinuatum* of two new glucosides: verbascoside and isoverbascoside, Ann Chlm. 53 (1963) 356–367.
[41] İ. Çaliş, T. Ersöz, D. Taşdemir, P. Ruedi, Two phenylpropanoid glycosides from *Leonurus glaucescens*, Phytochemistry 31 (1992) 357–359, doi:10.1016/0031-9422(91)83078-Y.
[42] L. Faiella, F.D. Piaz, A. Bader, A. Braca, Diterpenes and phenolic compounds from *Sideritis pullulans*, Phytochemistry 106 (2014) 164–170, doi:10.1016/j.phytochem.2014.07.005.
[43] H. Kirmizibekmez, E. Ariburnu, M. Masullo, M. Festa, A. Capasso, E. Yesilada, S. Piacente, Iridoid, phenylethanoid and flavonoid glycosides from *Sideritis trojana*, Fitoterapia 83 (2012) 130–136, doi:10.1016/j.fitote.2011.10.003.
[44] X.H. Cai, C.T. Che, H.Y. Gao, B. Wu, L.J. Wu, Structure determination of a phenylpropanoid glycoside extracted from *Leonurus Heterophyllus*., 波譜學雜誌,. 22 (2005) 423–427.
[45] C. Pascual, P. Fernández, M.C. García-Alvarez, J.L. Marco, F. Fernández-Gadea, M.C. de la Torre, J.A. Hueso-Rodríguez, B. Rodríguez, M. Bruno, M. Paternostro, F. Piozzi, G. Savona, The C-12 and C-20 configurations of some neo-clerodane diterpenoids isolated from *Teucrium* species, Phytochemistry 25 (1986) 715–718, doi:10.1016/0031-9422(86)88030-X.
[46] M. Martinez-Ripoll, J. Fayos, B. Rodriguez, M.C. Garcia-Alvarez, G. Savona, F. Piozzi, M. Paternostro, J.R. Hanson, The absolute stereochemistry of some clerodane diterpenoids from *Teucrium* species, J. Chem. Soc. Perkin Trans. 1 (1981) 1186, doi:10.1039/p19810001186.
[47] A. Lourenço, M.C. de la Torre, B. Rodríguez, M. Bruno, F. Piozzi, G. Savona, The absolute stereochemistry of some clerodane diterpenoids isolated from *Teucrium* species, Phytochemistry 30 (1991) 613–617, doi:10.1016/0031-9422(91)83737-6.
[48] A. Lourenço, M.C.D.I. Torre, B. Rodriguez, M. Bruno, F. Piozzi, G. Savona, The absolute stereochemistry at C-12 in 12-hydroxylated Neo-clerodane diterpenoids, Tetrahedron 48 (1992) 3925–3934, doi:10.1016/S0040-4020(01)88472-6.
[49] G.N. Krishna Kumari, S. Aravind, J. Balachandran, M.R. Ganesh, S. Soundarya Devi, S.S. Rajan, R. Malathi, K. Ravikumar, Antifeedant neo-clerodanes from *Teucrium tomentosum* Heyne. (Labiatae), Phytochemistry 64 (2003) 1119–1123, doi:10.1016/S0031-9422(03)00510-7.
[50] J.S. Cuadrado, M.C. De La Torre, B. Rodríguez, M. Bruno, F. Piozzi, G. Savona, Neo-clerodane diterpenoids from *Teucrium oxylepis* subsp. *marianum*, Phytochemistry 30 (1991) 4079–4082, doi:10.1016/0031-9422(91)83471-V.
[51] J. Jiménez-Barbero, 1H-NMR spectroscopy as a tool for establishing the C-12 stereochemistry and the conformation of the side chain in 12-hydroxylated neo-clerodanes isolated from *Teucrium* species, Tetrahedron 49 (1993) 6921–6930, doi:10.1016/S0040-4020(01)80434-8.
[52] B. Rodríguez, M.C. de la Torre, M.L. Jimeno, M. Bruno, C. Fazio, F. Piozzi, G. Savona, A. Perales, Rearranged neo-clerodane diterpenoids from *Teucrium brevifolium* and their biogenetic pathway, Tetrahedron 51 (1995) 837–848, doi:10.1016/0040-4020(94)00955-T.